Research & Reviews: Journal of Material Sciences
DOI: 10.4172/2321-6212.1000169

e-ISSN: 2321-6212
p-ISSN: 2347-2278

Synthesis of Monodispersed TiO2 Nanosheets by Wet Chemical Method and their Applications in Dye-Sensitized Solar Cells

Prakash T[1*], Navaneethan M[2], Archana J[3], Ponnusamy S[4], Muthamizhchelvan C[4] and Hayakawa Y[2]

[1]QIS Institute of Technology, Department of S & H, Ongole, Prakasm, Andhra Pradesh, India

[2]Research Institute of Electronics, Shizuoka University, 3-5-1 Johoku, Naka-ku, Hamamatsu, Shizuoka, Japan

[3]Research Institute, Department of Physic & Nanotechnology, SRM University, Kattankulathur, Kancheepuram, Tamil Nadu, India

[4]Department of Physics & Nanotechnology, SRM University, Kattankulathur, Kancheepuram, Tamil Nadu, India

Research Article

Received: 08/05/2017
Accepted: 24/05/2017
Published: 30/05/2017

***For Correspondence**

Prakash T, QIS Institute of Technology, Department of S & H, Ongole, Prakasm, Andhra Pradesh, India, Tel: 7093088103.

Email: t.prakash.phy@gmail.com

Keywords: Nanosheets, Nanomaterials, Semiconductors

ABSTRACT

Anatase TiO_2 nanosheets were prepared by wet chemical method in the presence of Tripropylamine as capping ligand. The obtained samples were characterized by Powder X-ray diffraction, Raman spectroscopy, Ultraviolet-visible spectroscopy, Fourier transform infrared spectroscopy, Field emission scanning electron microscopy, Transmission electron microscopy and high-resolution transmission electron microscopy. The growth mechanism for the formation of TiO_2 nanosheet has been investigated. The photovoltaic properties of anatase TiO_2 nanosheets were investigated by assembling the TiO_2 nanosheets as photoanodes in dye-sensitized solar cells (DSSCs). Experimentally, it shows that the anatase phase of TiO_2 nanosheet films have conversion efficiency of 3.25%.

INTRODUCTION

Titanium dioxide (TiO_2) is a widely studied metal oxide. When serving as the anode material for Dye sensitized solar cell (DSSCs), TiO_2 delivers higher conversion efficiency when compared to that of other semiconducting materials [1-5]. It's most significant advantage is the ability to adsorb more number of dye molecules with less dye aggregation [6-13]. Even though conversion efficiency of TiO_2, is not enough. So proper nanostructure engineering is required to achieve the high conversion efficiency in DSSCs. Moreover, such a strategy also appears to be effective in improving the DSSCs of TiO_2 [14-19]. Yang et al. synthesized anatase single crystals of TiO_2 with 47% of the highly reactive {0 0 1} facets by using hydrofluoric acid (HF) as a capping agent under hydrothermal conditions [20]. Yang et al. reported a new solvothermal method using 2-propanol as a synergistic capping agent and reaction medium together with HF to synthesize high-quality anatase TiO_2 single-crystal nanosheets (SCNSs) with 64% of the {0 0 1} facets [21]. Guo et al. synthesized anatase TiO_2 nanosheets by using hydrofluoric acid (HF) as a capping agent under hydrothermal conditions [22]. Wang et al. have represented hierarchically structured spheres consisting of ultrathin nanosheets by using hydrothermal method and achieved the power conversion efficiency of 4.66% without any $TiCl_4$ treatment [23]. Fortunately, the recently discovered anatase TiO_2 nanosheets (NSs) demonstrate the conversion efficiency upto 8% [24]. With the aim of obtaining enhanced photoanode performance, many studies on different modifications of TiO_2 have been performed [20]. Moreover, during the last few years, an increasingly great number of TiO_2 nanosheet structure has been synthesized and tested as possible alternatives to other TiO_2 nanostructures to improve its light to electric conversion efficiency in DSSCs with templates as shape controllers. In our previous reports, TEA was used as capping ligand to obtain size confined monodispersed nanoparticles of CdS and PbS [25,26]. Hexamethylenetetramine was used as capping ligand to obtain ZnO nanosheets for dye sensitized solar cell characteristics [27].

Research & Reviews: Journal of Material Sciences
DOI: 10.4172/2321-6212.1000169
e-ISSN: 2321-6212
p-ISSN: 2347-2278

In the present work, TiO_2 nanosheets were synthesized by simple wet chemical method using tripropylamine (TPA) as a capping ligand at low temperature without any templates. Further, photo anodes were successfully fabricated using TiO_2 nanosheets and the cell performances were characterized.

MATERIALS AND METHODS

Synthesis of TiO_2 nanosheets

All chemicals were purchased from Wako chemicals (Japan) and used without further purification. 0.5 mL of tripropylamine (TPA) was added slowly to 40 mL ethanol under vigorous stirring. 4 mL titanium isopropoxide (TIP) was then added drop wise to the parent solution under vigorous stirring. A white precipitate was obtained after few minutes. The ratios of titanium isopropoxide (TIP), tripropylamine (TPA) and ethanol in the above solution were 4:0.5:40. The reaction was continued for 12 h at room temperature. Finally, the precipitates were washed with water for several times and dried at 100°C for 12 h and it was labelled as S2. The same preparation procedure was followed for the preparation of uncapped sample without TPA and it was labelled as S1.

Dye sensitized Solar cell fabrication

Firstly, 2 g of TPA capped TiO_2 nanosheets was dispersed in 50 ml of ethanol and this mixture was ground in a mortar for a few minutes to form colloidal suspensions. Then, 5 drops of triton-X were added to the solution as an organic binder. Fluorine doped tin oxide (FTO) substrates were cleaned ultrasonically using a mixture of acetone and ethanol for 30 minutes. The TiO_2 colloidal solutions were sprayed over the FTO substrate at a substrate temperature of 150°C by spray deposition method. TPA capped TiO_2 nanosheets coated FTO substrates (photoanodes) were successively sintered at 530°C for 2 h. Sintered FTO photoanodes were sensitized with ruthenium [0.03 M di-tetrabutylammoniumcis–bis (isothiocyanato) bis (2,2″-bipyridyl-4,4′-dicarboxylato) ruthenium (II) (N-719)] solution in ethanol. The dye-sensitized photoanode and Pt-coated counter electrode were clamped using clips. Finally, an iodide based redox electrolyte was filled between the electrodes via capillary action.

Measurement techniques

Phase identification was done by the powder X-ray diffraction, using Rigaku X-ray diffractometer with Cu Ka radiation at 0.02°/s step interval. Raman spectra were obtained using a JASCO NR 1800 Raman spectrophotometer equipped with Nd:YAG laser. UV–visible absorption analyses were performed using a Shimadzu (Japan) 3100 PC spectrophotometer with ethanol as dispersing medium. Fourier transform infrared (FTIR) spectra were obtained from JEOL JIR-WINSPEC 50 spectrometer. The morphology of the samples was observed through transmission electron microscopy (JEOL JEM 2100F, Japan) and field emission scanning electron microscopy (FESEM, JEOL JSM 6320F, Japan). Photocurrent–voltage measurements were performed under AM1.5 100 mW/cm^2 simulated light irradiation (YSS-80A, Japan) using a Xe lamp as the light source equipped with an infrared (IR) filter.

RESULTS AND DISCUSSION

Figure 1 shows the XRD patterns of uncapped and TPA capped TiO_2 powder samples S1 and S2 respectively. XRD patterns of uncapped S1 sample show the amorphous nature of TiO_2 powder. XRD patterns of TPA capped S2 sample show the anatase phase of TiO_2 powder (JCPDS Card no. 78-2486). The width of XRD diffraction peaks of anatase becomes broad, indicating the formation of greater TiO_2 crystallites and enhancement of crystallization. The TEM images of S2 sample are shown in below figures. It can be clearly shown that the growth of crystalline TiO_2 nanocrystals is in concurrence with the experiment results of XRD (Figure 1).

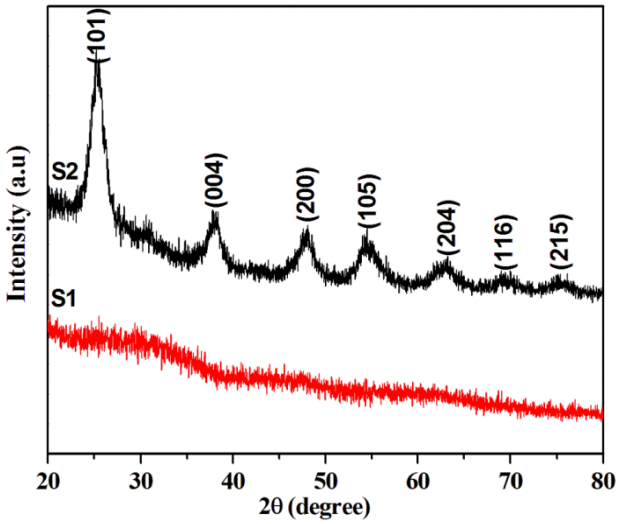

Figure 1. XRD patterns of uncapped TiO_2 nanoparticles (S1) and TPA capped TiO_2 nanosheets (S2).

Research & Reviews: Journal of Material Sciences
DOI: 10.4172/2321-6212.1000169
e-ISSN: 2321-6212
p-ISSN: 2347-2278

To investigate the crystalline phase of TiO_2 and quality of sample, Raman spectroscopy was applied as a powerful tool to detect the significant structural changes in TiO_2 during the wet chemical reaction process. The Raman spectra (Figure 2) show remarkable difference due to amorphous (uncapped) and crystalline material (TPA capped) of TiO_2. Uncapped (S1) TiO_2 nanoparticles do not show any mode of vibration because the sample was in amorphous nature. Four representative modes of E_g (151 cm^{-1}), $B1_g$ (404 cm^{-1}), $A1_g$ (517 cm^{-1}) and E_g (640 cm^{-1}) are the same as the modes of anatase TiO_2 TPA capped (S2) nanosheets. The results confirm that the phase of TiO_2 sheets is in agreement with XRD analysis [28].

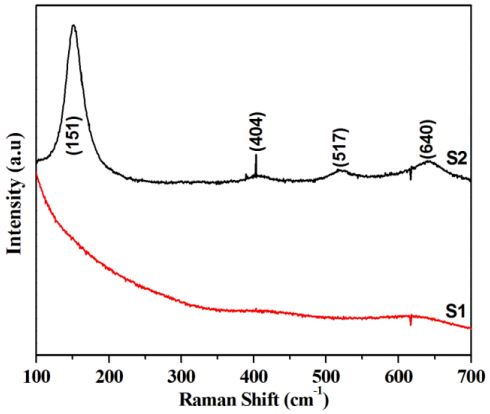

Figure 2. Raman spectra of uncapped TiO_2 nanoparticles (S1) and TPA capped TiO_2 nanosheets (S2).

The absorption spectra (Figure 3) reveal that the absorption edges of TPA capped (S2) sample shifted towards blue region compared to uncapped (S1) TiO_2 sample. The absorption edge of uncapped TiO_2 observed is at 360 nm and that for TPA capped observed 340 nm. These differences in UV spectra reveal the possibility of the structural change such as reduction in the size.

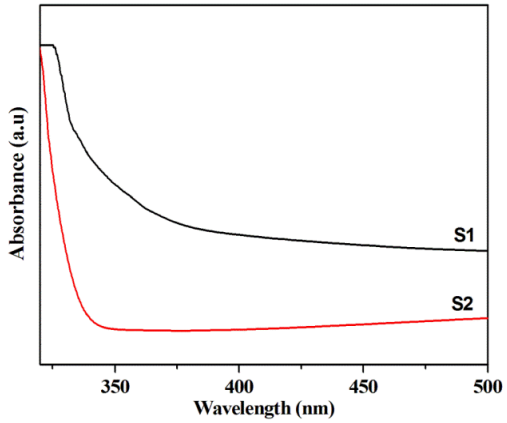

Figure 3. UV spectra of uncapped TiO_2 nanoparticles (S1) and TPA capped TiO_2 nanosheets (S2).

FTIR spectrum of TPA capped (S1) and uncapped (S2) samples of TiO_2 are presented in Figure 4. Absorption in the low wavenumber region between 1000–900 cm^{-1} is typically assigned to O–Ti–O bond in crystalline TiO_2 [29]. FTIR band at 2365 cm^{-1} can be assigned to C-O vibration. The bands in the 3000–3500 cm^{-1} range are attributed to OH vibration on the surface of TiO_2 from the environment [29]. FTIR bands in the 1393 cm^{-1} and 1623 cm^{-1} are due to N-H vibration of TPA [30]. It clearly demonstrates the surface passivation of TPA molecule on the surface of TiO_2 nanoparticles.

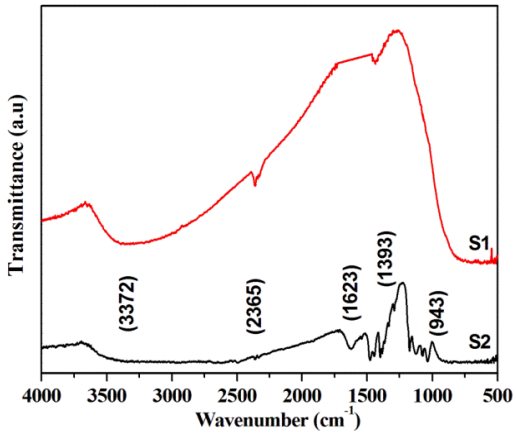

Figure 4. FTIR spectra of uncapped TiO_2 nanoparticles (S1) and TPA capped TiO_2 nanosheets (S2).

Research & Reviews: Journal of Material Sciences
DOI: 10.4172/2321-6212.1000169
e-ISSN: 2321-6212
p-ISSN: 2347-2278

Based on the morphological studies, the formation mechanism of TPA capped TiO_2 nanosheet is explained as follows: lone pair of electrons in the nitrogen atom of TPA was attached to the surface of the TiO_2 nanoparticles due to the affinity of the nitrogen with Ti^{4+}. The nitrogen atom forms a co-ordinate bond with the surface of TiO_2 because of its chemisorption properties. In addition to that, the longer growth time and alcoholysis of TPA in the presence of ethanol resulting the formation of nanosheets. The addition of TPA molecules to the titanium hydroxyl ions restricts further growth of the c-axis owing to the chemisorption or adsorption of amine molecules on the surface. Finally, annealing at 100°C leads to the formation of TiO_2 nanosheets.

The morphology analyses of uncapped and TPA capped TiO_2 samples were carried out using FESEM and TEM as shown in Figure 5. Uncapped sample have shown that spherical morphology with more agglomeration. Nanosheets like morphology was exhibited by TPA capped samples with crystalline quality. Wang et al. [31] synthesized TiO_2 nanosheets with a typical thickness of 97 nm with average diameter of about 493 nm and length 520 nm. TiO_2 nanosheets with a typical thickness of 260 nm average diameter about 1.09 μm were synthesized by Yang et al. [21]. Guo et al. [22] synthesized TiO_2 nanosheets with a typical thickness of 40-60 nm and length 500-800 nm. In the present work, TiO_2 nanosheets of average diameter and length are 150 nm and 250 nm, respectively. Moreover, TiO_2 nanosheets were synthesized by using TPA as a capping ligand with high monodispersity. From this, one can conclude that TPA acted as effective capping ligand for TiO_2 nanosheets synthesis by the simple chemical method. High resolution transmission electron microscopy (HRTEM) showed lattice fringes and indicates that TPA capped TiO_2 nanosheets were crystalline. The schematic representation for synthesizing TiO_2 nanosheets is shown in Figure 6.

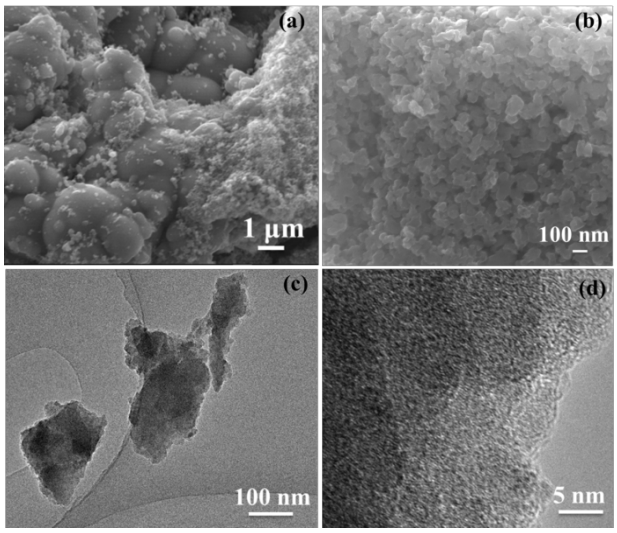

Figure 5. FESEM and TEM images of uncapped (a) TiO_2 nanoparticles and TPA capped TiO_2 nanosheets (b-d).

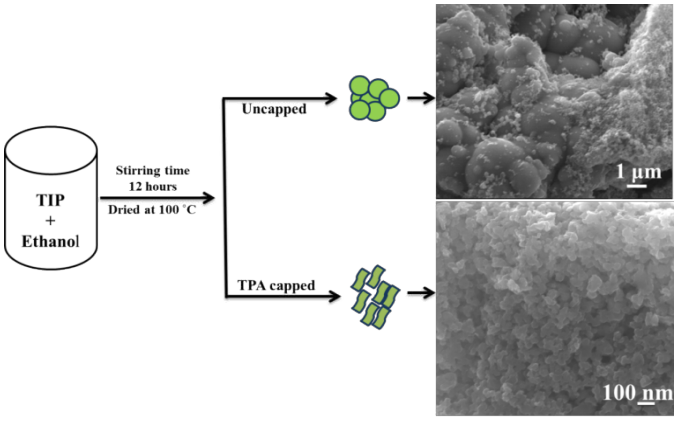

Figure 6. Formation mechanism of TiO_2 nanostructures.

Figure 7 shows the I-V characteristics for dye sensitized solar cell which was fabricated by the TiO_2 films prepared with nanosheets for sample S2. The current-voltage curves reveal that the DSSC prepared based on the synthesized TiO_2 nanosheets presents less short-circuit current (Jsc) over that of the reports already published [32]. The DSSC which was fabricated based on the as synthesized TiO_2 nanosheets shows J_{sc}=6.55 mA/cm^2 and V_{oc}=0.79 V with the power conversion efficiency (PCE) of 3.25%, respectively, whereas the DSSC based on anatase TiO_2 nanosheets based microspheres J_{sc}=15.2 mA/cm^2 and V_{oc}=0.65 V with the power conversion efficiency (PCE) of 6.64%, respectively, indicating 50% decrease in J_{sc} and PCE compared to the reported results [32]. It is well-known that an increase in the light-scattering ability plays an important role in the light-harvesting efficiency and Dye adsorption ability. Compared to the monodispersed anatase TiO_2 nanosheets, nanosheets-based microspheres have more ability to absorb more amounts of dye molecules due to the porous nature of the microsphere. Light-scattering ability and amount of

e-ISSN: 2321-6212
p-ISSN: 2347-2278

dye adsorption, these are the two important factors for the less power conversion efficiency for as synthesized TiO_2 nanosheets. However, as synthesized TiO_2 nanosheets preparation procedure is very simple compared to the published report [32].

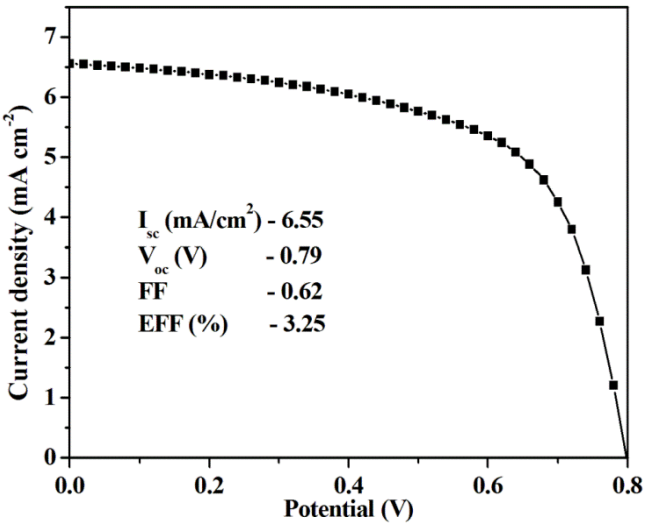

Figure 7. I-V curve of TPA capped TiO_2 nanosheets (S2).

There have been, over the past decades, a number of synthetic routes to the preparation of TiO_2 nanostructures. For example, conventional hydrolytic sol-gel process and emulsion precipitation [33-36] performed at relatively low temperature yield amorphous products with polydisperse particles, and subsequent calcination is needed to induce crystallization. We presented a simple growth process for fabrication of TiO_2 nanosheets in ethanol solution at low temperature. The results indicate that monodispersed crystalline TiO_2 nanosheets in large scale have been successfully synthesized by chemical method. Meanwhile, the morphology of crystalline TiO_2 nanosheets easily controlled using TPA as a capping ligand without further calcination.

CONCLUSIONS

Nanocrystalline anatase TiO_2 nanosheets were employed as a photoanode material in dye-sensitizedsolar cells. XRD and Raman spectra confirms the formation of anatase phase TiO_2 nanosheets. UV spectra confirm the TPA capped sample shifted towards blue region compare to that of uncapped sample. FTIR spectra confirm the passivation of TPA on surface of the TiO_2. FESEM and TEM results confirm the TPA capped sample with monodispersity and crystalline quality. The efficiency of the cell using TiO_2 nanosheets was about 3.25%.

REFERENCES

1. Regan B and Grätzel M. A low-cost, high-efficiency solar cell based on dye-sensitized colloidal TiO_2 films. Nature 1991;353:737-740.
2. An BK, et al. Ruthenium complex-c ored dendrimers: Shedding light on efficiency trade-offs in dye-sensitised solar cells. Meredith Org Electron 2009;10:1356-1363.
3. Robertson N. Optimizing Dyes for Dye-Sensitized Solar Cells. Angew Chem Int Edit 2006;45:2338-2345.
4. Zhang Q, et al. Aggregation of ZnO Nanocrystallites for High Conversion Efficiency in Dye-Sensitized Solar Cells. Angew Chem Int Edit 2008;47:2402-2406.
5. Chen D, et al. Mesoporous Anatase TiO_2 Beads with High Surface Areas and Controllable Pore Sizes: A Superior Candidate for High-Performance Dye-Sensitized Solar Cells. Adv Mater 2009;21:2206-2210.
6. Wu X, et al. Solar Cells: Nanosized Anatase TiO_2 Single Crystals with Tunable Exposed (001) Facets for Enhanced Energy Conversion Efficiency of Dye-Sensitized Solar Cells. Adv Funct Mater 2011;21:4166.
7. Wu X, et al. Shell-in-shell TiO_2 hollow spheres synthesized by one-pot hydrothermal method for dye-sensitized solar cell application. Energy Environ Sci 2011;4:3565-3572.
8. Wu X, et al. Amino acid assisted synthesis of mesoporous TiO_2 nanocrystals for high performance dye-sensitized solar cells. J Mater Chem 2012;22:10438-10440.
9. Fan J, et al. Enhanced photovoltaic performance of dye-sensitized solar cells based on TiO_2 nanosheets/graphene composite films. J Mater Chem 2012;22:17027-17036.
10. Li TC, et al. Ni(III)/(IV) Bis(dicarbollide) as a Fast, Noncorrosive Redox Shuttle for Dye-Sensitized Solar Cells. J Am Chem Soc 2010;132:4580-4582.

e-ISSN: 2321-6212
p-ISSN: 2347-2278

11. Grätzel M. Recent advances in sensitized mesoscopic solar cells. Acc Chem Res 2009;42:1788-1798.

12. Kavan L, et al. Optically Transparent Cathode for Dye-Sensitized Solar Cells Based on Graphene Nanoplatelets. ACS Nano 2011;5:165-172.

13. Gomez DAL, et al. Thompson ME and Zhou C. A Continuous, highly flexible, and transparent graphene films by chemical vapor deposition for organic photovoltaics. ACS Nano 2010;4:2865-2873.

14. Sommeling PM, et al. Influence of a $TiCl_4$ post-treatment on nanocrystalline TiO_2 films in dye-sensitized solar cells. J Phys Chem B 2006;110:19191-19197.

15. Yu H, et al. An efficient and low-cost TiO_2 compact layer for performance improvement of dye-sensitized solar cells. Electrochim Acta 2009;54:1319-1324.

16. Herman GS, et al. Experimental Investigation of the Interaction of Water and Methanol with Anatase-TiO_2 (101). J Phys Chem B 2003;107:2788-2795.

17. Vittadini A, et al. Structure and Energetics of Water Adsorbed at TiO_2 Anatase 101 and 001 Surfaces. Phys Rev Lett 1998;81:2954

18. Yu J, et al. Anatase TiO_2 nanosheets with exposed (001) facets: improved photoelectric conversion efficiency in dye-sensitized solar cells. Nanoscale 2010;2:2144-2149.

19. Liu S, et al. Anatase TiO_2 with Dominant High-Energy {001} Facets: Synthesis, Properties, and Applications. Chem Mater 2011;23:4085-4093.

20. Yang HG, et al. Anatase TiO_2 single crystals with a large percentage of reactive facets. Nature 2008;453:638-641.

21. Yang HG, et al. Solvothermal Synthesis and Photoreactivity of Anatase TiO_2 Nanosheets with Dominant {001} Facets. J Am Chem Soc 2009;131:4078-4083.

22. Guo W, et al. Direct Growth of TiO_2 Nanosheet Arrays on Carbon Fibers for Highly Efficient Photocatalytic Degradation of Methyl Orange. Adv Mater 2012;24:4761-4764.

23. Wang H, et al. Reduced electron recombination of dye-sensitized solar cells based on TiO_2 spheres consisting of ultrathin nanosheets with [001] facet exposed. Beilstein J Nanotechnol 2012;3:378-387.

24. Zhou H, et al. Anatase TiO_2 nanosheets with exposed highly reactive (001) facets as an efficient photoanode for quantum dot-sensitized solar cells. RSC Adv 2016;6:67968-67975.

25. Nisha KD, et al. Inorganic surface passivation of CdS nanocrystals resulting in strong luminescence. J Alloy Compd 2009;486:844-847.

26. Navaneethan M, et al. Optical and surface morphological properties of triethylamine passivated lead sulphide nanoparticles. Mater Chem Phys 2009;117:443-447.

27. Navaneethan M, et al. Functional properties of amine-passivated ZnO nanostructures and dye-sensitized solar cell characteristics. Chem Eng J 2012;213:70-77.

28. Wang DH, et al. One-step hydrothermal synthesis of N-doped TiO_2/C nanocomposites with high visible light photocatalytic activity. Nanoscale 2012;4:576-584.

29. Ryskin YI. The Infrared Spectra of Minerals. In: Farmer VC (ed.) Mineralogical Society, London, 1974.

30. Zhang R and Gao L. Synthesis of nanosized TiO_2 by hydrolysis ofalkoxide titanium in micelles. Key Eng Mater 2002;573:224-226.

31. Wang WS, et al. Large Ultrathin Anatase TiO_2 Nanosheets with Exposed {001} Facets on Graphene for Enhanced Visible Light Photocatalytic Activity. J Phys Chem C 2012;116:19893-19901.

32. Wang Y, et al. Preparation and Characterization of Anatase TiO_2 Nanosheets-Based Microspheres for Dye-Sensitized Solar Cells. Ind Eng Chem Res 2011;50:11982-11987.

33. Sugimoto T, et al. Synthesis of uniform anatase TiO_2 nanoparticles by gel-sol method. 4. Shape control. J Colloid Interface Sci 2003;259:53-61.

34. Kanie K and Sugimoto T. Shape control of anatase TiO_2 nanoparticles by amino acids in a gel-sol system. Chem Commun 2004;1584-1585.

35. Lin J, et al. Hot-Fluid Annealing for Crystalline Titanium Dioxide Nanoparticles in Stable Suspension. J Am Chem Soc 2002;124:11514-11518.

36. Murakami Y, et al. Salt Catalysts Containing Basic Anions and Acidic Cations for the Sol−Gel Process of Titanium Alkoxide: Controlling the Kinetics and Dimensionality of the Resultant Titanium Oxide. J Phys Chem B 1999;103:1836-1840.